A ROBUST CONTROLLER DESIGN FOR AN INLET THROTTLING SPEED CONTROL SYSTEM FOR A ROTARY ACTUATOR

Aws M. Abdullah[1][0000-0003-1956-1476], Hasan H. Ali[2], Arif A. Al-Qassar[3]*
[1]University of Baghdad, Baghdad, Iraq
[2]Directorate of Studies, Planning, and Follow-up, Ministry of Higher Education and Scientific Research, Baghdad, Iraq
[3]Control and Systems Engineering Department, University of Technology, Baghdad, Iraq
Email: aws.abd@cois.uobaghdad.edu.iq

Abstract - In this paper, a novel flow control strategy which is the inlet throttled pump was used to design an angular velocity control system for rotary actuator. Inlet throttled systems have good performance in addition to their high efficiency compared to traditional valve-controlled systems. The flow in the proposed system is adjusted by a valve that is positioned at the pump inlet with the purpose of reducing the energy loses across the valve. This regulated flow is used then to control the actuator angular velocity. The system was modeled and the open loop stability and performance were studied. In order to improve the system performance, proportional-integral-derivative (PID) and H-infinity controllers have been designed. The multiplicative uncertainty was analyzed to assess the robustness of the feedback control system where six parameters were considered uncertain within a range of ±10%. The robust stability and performance requirements of the closed-loop angular velocity control system were assessed in the frequency domain. The time response of the system showed that the system is stable with both PID and H-infinity controllers. The PID controller have the advantages of simplicity and high response speed while the H∞ controller provides better nominal performance, robustness, and stability. The H∞ controller can handle parametric uncertainty without requiring pure integral term which is a significant advantage over the PID controller. On the other hand, the PID controller falls short of achieving robust performance, making it less suitable for systems that require high levels of performance and robustness. In summary, the H∞ controller is a more comprehensive solution for ensuring the best performance of a system. In contrast, the PID controller may be more suitable for systems with less stringent performance requirements.

Keywords: Pump, Valve, Inlet throttling valve, Angular velocity control, Robust control.

1. Introduction

A hydrostatic transmission (HST) system is proposed in this paper. The (HST) converts mechanical power into hydraulic power (flow and pressure) in the place of power generation and reconverts it into mechanical power at the output drive shaft. It transmits mechanical power from one place to another without using gears [1]. The (HST) could remain stalled and undamaged under full load conditions with less maintenance required to keep the system operative comparatively. This proposed (HST) consists mainly of the inlet-throttled pump and a throttling valve for adjusting the pump flow rate and a rotary actuator as shown in Fig. 1. The pump sends its flow towards a rotary actuator, which is responsible for converting hydraulic energy into rotational motion. This mechanism is commonly used in various industrial applications, such as airplanes, heavy duty vehicles, robotic arms and conveyor systems, to perform precise and controlled movements. The 4-way valve changes the flow direction to the actuator when a change in the motion of the actuator is required. The inlet throttling valve is positioned at the inlet of the pump to reduce the energy losses across it [2,3]. In robust control, the system must remain stable with pre-specified performance despite variations in operating conditions and uncertainties.

Many studies have been conducted on the hydrostatic transmissions and improving stability and performance of the hydrostatic transmission. Uncertainty of the inlet metering velocity control system was proposed in [4]. In that work, PID and H∞ were designed. The results showed that the performance of the system with H-infinity and PID controllers is almost the same. However, only H-infinity controller meets the requirements of robustness. In [5], a motion control system for a linear hydraulic actuator was studied. A feedforward plus PID (FPID) controller has been used for adjusting the flow through a directional metering

valve and compensating the system's nonlinearity. While the PID controller manages the error signal, the FPID controller improved the system stability and performance.

A hydraulic system that uses a variable speed pump to control the speed of a hydraulic motor is presented in [6]. A mathematical model was established to evaluate the performance and stability of the open-loop system. After that, PID and the H-infinity controllers have been proposed to improve system performance while comparing in terms of system stability and system performance improvement. In [7], a new hydraulic circuit was developed in which the pump was replaced with a new electro-hydraulic one for optimizing the operational points. This new system was utilized in a prototype agriculture tractor of medium segment. The controller design process was based on robust H∞ optimization techniques for improving the robust stability and performance of the system. An H∞ based robust control design combined with feedback linearization for an automatic bucket leveling mechanism of a wheel loader was presented in [8]. A multi-input-multi-output nonlinear dynamic model of wheel loader that is electro-hydraulically actuated was established. The controller robustness was verified through the system analysis and simulation based on the nonlinear dynamic model of the system.

In [9], a decentralized H-infinity loop-shaping controller a two-area deregulated non-reheat thermal power system was proposed. The controller could achieve the feedback performance aims by shaping the open loop gain with a precise dynamic response, reference response and disturbance rejection at low frequencies and system robustness. A conventional hydraulic transmission consisting of a variable displacement pump and a constant displacement motor was studied in [10]. Multiplicative and additive uncertainties were considered to identify uncertainty models which can be considered for robustness analysis of systems while applying feedback control. PID and H∞ controllers are designed to control the position and velocity of the system. In [11], a speed control system using an inlet throttling valve-controlled pump was proposed. To improve the stability and performance of the system, the stability and performance of open and closed loop speed control systems have been investigated using PID, H∞, and multi-degrees of freedom controllers. In [12] a robust control strategy was presented to control the attitude of a missile whose fins are actuated from its deflection by the autopilot. In that work, the authors stabilized the rotational motion of the missile while correcting the angle of attack. Multi-degrees of freedom H-∞ control strategy was implemented for the pitch rate adjustment problem. The results were compared to the H-∞ controller design method. An investigation on the optimization and real-time design of the H∞ controller for systems with uncertainties was proposed in [13]. Ring modulation control with mixed sensitivity control functionality is implemented such way that ensures system robustness of the system with nonlinearities.

In [14], a new technique of multi-degrees of freedom H-infinity Control for DC Motor was presented. This proposed method applied the genetic algorithms to satisfy the required structure robust control system. The achieved system robustness of proposed multi-degrees of freedom control design was compared with the typical multi-degrees of freedom H-infinity controller. That strategy was shown to be simpler with a lower order compared to that of the typical control method. A control system which is utilized to manipulate the speed of a hydraulic actuator with uncertainty consideration in the system parameters was presented in [15]. The dynamics of the system was modeled and the open loop system response has been assessed. Various controllers (PID and H-infinity) have been considered to investigate the response of the feedback system and a comparison has been made against the open loop circuit. The uncertain system robustness was examined. In [16], a new design procedure for two degrees of freedom (TDF) controllers was introduced. The feedback and the pre-filter controllers have been proposed in a one step in an H-infinity (H∞) optimization strategy. The controller was implemented to satisfy the robustness and disturbance rejection characteristics, while the pre-filter controller was implemented for shaping the feedback control system response.

In this work, a speed control system for a hydraulic motor was designed. A throttling valve along with a constant displacement pump was used as a means of flow adjustment. The system was modeled and stability and performance of the open loop and feedback system cases have been investigated. For the closed loop case, PID and H-infinity controllers were considered and the frequency domain was adopted in the design process. The multiplicative parametric uncertainty was considered and the system robustness was assessed. The time response for the open and the feedback cases was determined and compared.

2. System Description

The diagram in Fig. 1 shows the proposed hydrostatic transmission that consists of a throttling valve, a fixed displacement pump, a 4-way directional valve and a rotary actuator. The flow is controlled using the throttling valve. The throttling valve is connected to the intake side of the fixed displacement pump. A relief valve is installed at the input supply pressure (P_{in}) side to regulate the pressure in the input line of the throttling valve. The standard four-way directional valve controls the

direction of the hydraulic fluid flow to the rotary actuator. The system load can be modeled as a rotary mass-spring-damper system with a load disturbance torque (T). Fig. (1) depicts the moment of inertia (J), torsional spring rate (k), and viscous drag coefficient (b) for the load. The rotary actuator which is connected to the output shaft has a volumetric displacement (V_a) and angular velocity (ω_a).

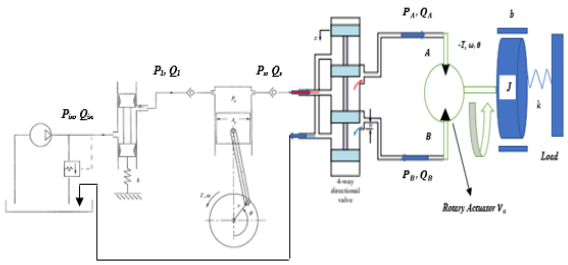

Figure 1: Inlet Throttling Velocity Control System for a Rotary Actuator

3. Modelling and Analysis

The governing equations of the system are derived and non-dimensionalised. They include the rotary actuator's motion equation (torque dynamics) and the equation of the rate of change of the pressure (pressure dynamics).

1-The torque dynamics can be expressed as follows [17,18],

$$J\ddot{\theta} + b\dot{\theta} + k\theta = \eta_{at} V_a (P_A - P_B) - T_d \quad (1)$$

P_A and P_B : Fluid pressures on the input and output of the actuator, respectively.

T_d: Disturbance Torque

V_a: Volumetric displacement of the actuator

η_{at}: Actuator Torque Efficiency

J: The mass moment of inertia

b: Viscous Damping Coefficient

θ: angular displacement

$\dot{\theta}$: angular velocity

$\ddot{\theta}$: angular acceleration

Let $P_s = P_A - P_B$, let $P_s = P_A$, $\dot{\theta} = \omega_a$

Assuming the orifice of the directional valve is adds no restrictions on the fluid flow, a small pressure drops through the valve passages and the directional control valve is resulted which can be neglected.

In Eq. (1), the torque exerted on the load by the rotary actuator is given by $\eta_{at} V_a (P_A - P_B)$ where η_{at} is the torque efficiency of the actuator.

For steady-state conditions:

$$\ddot{\theta} = \dot{\theta} = 0; \quad T = 0; \quad P_s = 0;$$

The load spring is typically excluded from velocity control analysis, i.e. k=0 [17], and the rotor actuator is $\omega_a = \dot{\theta}$

$$J\ddot{\theta} + b\dot{\theta} = \eta_{at} P_s V_a - T_d \quad (2)$$

The pressure dynamics can be expressed as:

$$\frac{V}{\beta}\dot{P}_s + k_1 P_s = (Q_i - V_a\dot{\theta}) \quad (3)$$

$V = V_O + V_a\hat{\theta}$: instantaneous volume of the chamber

Where $\hat{\theta} = \pi$*(1-cos (360 $*$ θ))/2

V_O: Volume of the chamber when θ equals zero

β: Fluid bulk modulus of elasticity

Q_i : Volumetric flow rate from the charge pump

k_1 : Coefficient of leakage

V_a: Volumetric displacement per unit of rotation

$$\dot{P}_s = \frac{\beta}{V_O + V_a\hat{\theta}}(Q_i - k_1 P_s - V_a\dot{\theta}) \quad (4)$$

To simplify the pressure rise rate equation, it can be linearized under certain nominal conditions, which are:

$$\hat{\theta}_0 = \dot{\theta}_0 = Q_{i0} = P_{s0} = 0 \quad (5)$$

The equation for the rate of pressure rise can be described in its linear form as follows,

$$\dot{P}_s = \frac{\beta}{V_O}(Q_i - k_1 P_s - V_a\dot{\theta}) \quad (6)$$

Where the inlet flow, Q_{in}, can be expressed as follows,

$$Q_i = A_v C_d \sqrt{\frac{2P_i}{\rho}} \quad (7)$$

The mathematical model can be generalized and simplified by non-dimensionlization [8]. Eq. (2) and Eq. (6), can be non-dimensionalized using the following reference conditions:

$$\begin{aligned} P_s &= \hat{P}_s P_{sr} \\ \omega_a &= \hat{\omega}_a \omega_{ar} \\ A_v &= \hat{A}_v A_r \\ P_i &= \hat{P}_i P_{ir} \\ t &= \hat{t}\tau \end{aligned} \quad (8)$$

where τ is the time constant. The resulting dimensionless equations may be expressed as follows,

$$\frac{d(\hat{P}_s P_{sr})}{d(\hat{t}\tau)} = \frac{\beta}{V_o}\left(A_r C_d \sqrt{\frac{2P_{ir}}{\rho}}\hat{A}_v\sqrt{\hat{P}_i} - k_1\hat{P}_s P_{sr} - V_a\hat{\omega}_a\right) \quad (9)$$

multiply Eq. (9) by τ/P_{sr}

$$\hat{P}_s = \frac{\tau\beta}{V_o P_{sr}} A_r C_d \sqrt{\frac{2P_{ir}}{\rho}}\hat{A}_v\sqrt{\hat{P}_i} - \frac{\tau\beta}{V_o}k_1\hat{P}_s - \frac{\tau\beta\omega_r}{V_o P_{sr}}V_a\hat{\omega}_a \quad (10)$$

$$\text{Let } \tau = \frac{V_o}{\beta k_1} \quad (11)$$

Substituting Eq. (11) into Eq. (10) gives:

$$\hat{P}_s = \frac{V_o}{\beta k_1}\frac{\beta}{V_o P_{sr}} A_r C_d \sqrt{\frac{2P_{ir}}{\rho}} \hat{A}_v \sqrt{\hat{P}_i} - \frac{V_o}{\beta k_1}\frac{\beta}{V_o} k_1 \hat{P}_s - \frac{V_o}{\beta k_1}\frac{\beta \omega_r}{V_o P_{sr}} V_a \hat{\omega}_a \quad (12)$$

The non-dimensional pressure rise equation can finally be written as follows,

$$\hat{P}_s + \hat{P}_s = \xi_1 \hat{A}_v \sqrt{\hat{P}_i} - \xi_2 \hat{\omega}_a \quad (13)$$

Where the dimensionless groups ξ_1 and ξ_2 are defined in Eqs. (14) and (15) respectively.

$$\xi_1 = \frac{A_r C_d \sqrt{\frac{2P_{ir}}{\rho}}}{P_{sr} k_1} \quad (14)$$

$$\xi_2 = \frac{\omega_{ar} V_a}{k_1 P_{sr}} \quad (15)$$

Similarly, the non-dimensional motion equation can be derived as follows,

$$\hat{J}\frac{d(\hat{\omega}_a \omega_{ar})}{d(\hat{t}\tau)} + \hat{b}\hat{\omega}_a \omega_{ar} = \eta_{at}\hat{P}_s P_{sr} V_a - \hat{T}_d \quad (16)$$

Dividing eq. (16) by $\eta_{at} P_{sr} V_a$, the equation of motion can be expressed in its dimensionless form as follows:

$$\hat{J}\dot{\hat{\omega}}_a + \hat{b}\hat{\omega}_a = \hat{P}_s - \hat{T}_d \quad (17)$$

Where:

$$\hat{J} = \frac{J\omega_{ar}}{\eta_{at} P_{sr} V_a \tau}$$
$$\hat{b} = \frac{b\,\omega_{ar}}{\eta_{at} P_{sr} V_a} \quad (18)$$
$$\hat{V}_a = \frac{V_a}{V_a} = 1$$
$$\hat{T}_d = \frac{\hat{T}_d}{\eta_{at} P_{sr} V_a}$$

Eq. (13) and Eq. (17) can be re-arranged in state-space matrix form as follows,

$$\dot{x} = Ax + Bu \quad (19)$$
$$y = Cx + Du$$

$$x = [\hat{P}_s \quad \hat{\omega}_a]^T \quad (20)$$
$$u = [\hat{A}v \quad \hat{T}_d]^T$$

$$y = \hat{\omega}_a$$

$$\dot{x}_1 = -x_1 - \xi_2 x_2 + \xi 1\sqrt{\hat{P}_i}\, u_1 \quad (21)$$
$$\dot{x}_2 = \frac{1}{\hat{J}} x_1 - \frac{\hat{b}}{\hat{J}} x_2 - \frac{1}{\hat{J}} u_2$$
$$y = x_2$$

$$A = \begin{bmatrix} -1 & -\xi_2 \\ \frac{1}{\hat{J}} & -\frac{\hat{b}}{\hat{J}} \end{bmatrix}, B = \begin{bmatrix} \xi_1\sqrt{\hat{P}i} & 0 \\ 0 & -\frac{1}{\hat{J}} \end{bmatrix}, \quad C = [0 \quad 1], D = 0 \quad (22)$$

Routh–Hurwitz stability criterion was used in this work to assess the open loop system stability. In this criterion, the coefficients of the characteristic equation must be all positive. The implementation of the Routh–Hurwitz stability criterion is described below,

$$\det(sI - A) = S^2 + \left(\frac{\hat{b}}{\hat{J}} + 1\right)S + \left(\frac{\hat{b}+\xi_2}{\hat{J}}\right) = 0 \quad (23)$$

$$a_0 = 1 > 0$$
$$a_1 = \left(\frac{\hat{b}}{\hat{J}} + 1\right) > 0$$
$$a_2 = \left(\frac{\hat{b} + \xi_2}{\hat{J}}\right) > 0$$

All the coefficients of the characteristic equation being greater than zero, indicates a stable open loop system.

The mathematical model was transformed into transfer functions, as shown in Eq. (24) and Eq. (25). The transfer function that relates the input valve opening area to the output angular velocity of the motor is:

$$G = \frac{\hat{\omega}_{aA}}{\hat{A}v} = \frac{\xi_1 / \hat{J}}{S^2 + \left(\frac{\hat{b}}{\hat{J}}+1\right)S + \left(\frac{\hat{b}+\xi_2}{\hat{J}}\right)} \quad (24)$$

The system transfer function which relates the input disturbance torque to the output angular velocity of the motor is:

$$G_d = \frac{\hat{\omega}_{ad}}{\hat{T}_d} = \frac{-\frac{S+1}{\hat{J}}}{S^2 + \left(\frac{\hat{b}}{\hat{J}}+1\right)S + \left(\frac{\hat{b}+\xi_2}{\hat{J}}\right)} \quad (25)$$

The transfer function for the dynamics of the inlet throttling valve was experimentally determined and is shown in equation (26):

$$G_v(s) = \frac{\hat{A}_v}{\hat{V}_{in}} = \frac{\hat{k}_v e^{-s\hat{t}_d}\hat{\omega}_n{}^2}{S^2 + 2\xi\hat{\omega}_n S + \hat{\omega}_n{}^2} \quad (26)$$

Where $\hat{V}_{in}$ is the valve input signal in volts, $\hat{\omega}_n$ is the valve natural frequency, and ξ is the damping ratio of the valve. The time delay t_d can limit the closed-loop bandwidth frequency ω_b as shown in non-dimensional bandwidth frequency [27,28]:

$$\hat{\omega}_b < \frac{1}{\hat{t}_d} \quad (27)$$

Equation (28) shows the transfer function for the complete dynamics of the system.

$$G(s) = G_v(s) G_P(s) \quad (28)$$

The numerical values of the parameters in Eqs. (24) and (26) are illustrated in Table 1 as dimensionless quantities.

Table (1): dimensionless parameters

Quantity	Values	Quantity	Values
$\hat{J}$	5.84	ξ_2	8.89
$\hat{b}$	0.15	$\hat{\omega}_n$	5.31
$\hat{T}$	1	ξ	0.8
$\hat{A}v$	1	$\hat{t}_d$	0.24
η_{at}	0.95	$\hat{k}_v$	1.214
ξ_1	10		

4. Controller Design and Uncertainty Analysis

4.1 PID Controller design

The PID controller is a closed-loop feedback controller which is widely implemented in industrial control systems. It calculates the error signal as the difference between a desired set point and a measured process variable, and applies a correction to the process based on three terms: proportional, integral, and derivative. The Particle Swarm Optimization (PSO) is a search technique, was used in this work to find near optimal values for K_p, K_i and K_d parameters [21]. The values of the proportional, integral, and derivative terms that were determined in this work are: K_p = 0.01, K_i = 0.2534, K_d = 0. The PID controller transfer function is $0.01(1+\frac{25.34}{S}+0s)$.

4.2 H_∞ Controller Design

The H_∞ controller transfer function *K(s)* was determined using the standard H_∞ optimization controller synthesis technique [22]. Figure (2) demonstrates that the transfer function matrix of a system with external inputs ($\hat{R}$ and $\hat{T}_d$) and the outputs z_1 and z_2 can have its H_∞ norm minimized by the H_∞ controller transfer function *K(s)*.

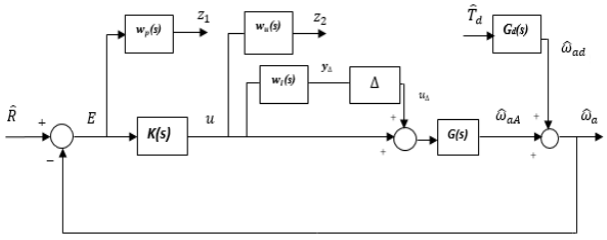

Figure 2: The proposed system block diagram with the weights

The performance weight, w_p, and the control effort weight, w_u, are frequency dependent weighting functions.

The performance weight in a control system is a function that is used to specify the desired performance of the system. It is a mathematical representation of the relative importance of different frequency components of the system's output.

The control effort weighting control function, $\boldsymbol{w_u}$, is a mathematical function that is used to assign different weights to different parts of a control system. This can be done to prioritize certain aspects of the system's performance, such as tracking accuracy or disturbance rejection. It can also be used to achieve reducing the control effort required to achieve the desired system performance, constraining the system states within a desired range and shaping the frequency response of the system. The performance weight is the inverse of the upper limit of the sensitivity transfer function frequency response. It is used to analyze the system performance. It is where it is calculated using Eq. (29) [23,24].

$$w_p = \frac{\frac{S}{M}+\hat{\omega}_b}{S+a\hat{\omega}_b} \tag{29}$$

The dimensionless bandwidth frequency is $\hat{\omega}_b$=0.105, with high frequency error M=1 and low frequency error a=10e-4. The gain was selected to be equal to 0.1 to ensure a reasonably small steady-state error. Larger gain leads to smaller steady-state errors but worse transient response.

In a non-dimensional model where parameters normalization is made about their maximum values, the control effort weight (w_u) is usually set to one, as illustrated in Fig. (2) [25].

The sensitivity function, S, is defined as the transfer function from the reference input, ($\hat{R}$), to the system error, (E), as shown in Fig. 3 and can be written as illustrated in Eq. (30).

$$S(s) = \frac{E(s)}{\hat{R}(s)}\frac{1}{1+G(s)G_c(s)} \tag{30}$$

The transfer function that describes the effect of the disturbance on the error signal is expressed as follows:

$$\frac{E(s)}{\hat{T}_d(s)} = -S(s).G_d(s) \tag{31}$$

The system's performance specification can be analyzed in terms of the required bandwidth of the sensitivity transfer function, the error value at high-frequency, and the error value at low-frequency using the frequency domain. **T**he H_∞ controller transfer function must be able to achieve the following conditions [22]:

$$|S.G_d(j\omega)| < \left|\frac{1}{w_P(j\omega)}\right|,\quad |S| < \left|\frac{1}{w_P(j\omega)}\right|,\quad |S.K| < \left|\frac{1}{w_u(j\omega)}\right|,\quad |S.K.G_d(j\omega)| < \left|\frac{1}{w_u(j\omega)}\right| \quad \forall\omega \tag{32}$$

$$z_1 = w_P\hat{R} - G_d w_P \hat{T}_d - G w_P u \quad (33)$$

$$z_2 = w_u u \quad (34)$$

$$E = \hat{R} - G_d \hat{T}_d - Gu \quad (35)$$

From the Eq. (33) to Eq. (35) as the matrices can be written as:

$$\begin{bmatrix} z_1 \\ z_2 \\ E \end{bmatrix} = \begin{bmatrix} w_P & -G_d w_p & -G w_p \\ 0 & 0 & w_u \\ 1 & -G_d & -G \end{bmatrix} \begin{bmatrix} \hat{R} \\ \hat{T}_d \\ u \end{bmatrix} \quad (36)$$

The generalized plant (P) is illustrated in Fig. (3):

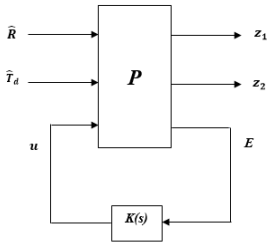

Figure 3: The generalized plant

A first-order Padé approximation was used to estimate the time delay of the valve. The transfer function of the H∞ Controller has been computed using the Matlab Function hinfsyn.m, as shown in Eq. (37).

$$K(s) = \frac{0.12\,s^6 + 1.407\,s^5 + 7.001\,s^4 + 15.35\,s^3 + 16.42\,s^2 + 11.95\,s + 0.0001258}{s^7 + 11.93\,s^6 + 60.7\,s^5 + 139.3\,s^4 + 162.5\,s^3 + 121.1\,s^2 + 0.002549\,s + 1.342e{-}08} \quad (37)$$

The variations of the parameters were considered in the overall system dynamics over a known range. The previous transfer functions will be used to generate perturbed plants to analyze the multiplicative uncertainty. The perturbed plants are used for defining the model of multiplicative uncertainty that is represented by the multiplicative uncertainty model as shown in Eq. (39) as well as uncertainty weight $w_I(j\omega)$ as shown in Eq. (40).

$$l_I(\omega) = max \left| \frac{G_{pert}(j\omega) - G(j\omega)}{G(j\omega)} \right| \quad (38)$$

$$w_I(j\omega) \geq l_I(\omega), \forall\omega \quad (39)$$

The multiplicative uncertainty was analyzed depending on six uncertain parameters, four of which are related to the dynamics of the throttling valve which are natural frequency, static gain, damping ratio, and time delay. These parameter changes were considered within the range of (+/−) 10% of their nominal values. On the other hand, the other two uncertain parameters are related to the dynamics of the rest of the system which are the discharge coefficient and the fluid bulk modulus with the range of (+/−) 10% of their nominal values. To ensure accuracy, the value of w_I should exceed the largest error l_I that occurs across the frequency domain.

The multiplicative error in Equation (38) has an upper bound which was obtained numerically by calculating the nominal plant $G(j\omega)$ and its perturbations, $G_{pert}(j\omega)$, for various frequency domains. The transfer function of the uncertainty weight, w_I, which represented the upper limit of the uncertainty as stated in Equation (39), is represented in red color in Fig. 10 and can be found in Equation (40).

$$w_I(s) = \frac{1.056\,S^2 + 12.47\,S + 27.92}{S^2 + 11.68\,S + 26.87} \quad (40)$$

The multiplicative uncertainty weight, w_I, the performance weight, w_p, and the control effort weight, w_u transfer functions are shown in Fig. (2). The signals, z_1 and z_2, are related to the performance weight, w_p, and the control effort weight, w_u, transfer functions, respectively. Based on Fig. 2, the equations may be written as follows,

$$y_\Delta = w_I u \quad (41)$$

$$z_1 = -G w_P u_\Delta + w_P\hat{R} - G_d w_P \hat{T}_d - G w_P u \quad (42)$$

$$z_2 = w_u u \quad (43)$$

$$E = -G u_\Delta + I\hat{R} - G_d \hat{T}_d - Gu \quad (44)$$

From eq. (41) to eq. (44) can be expressed in matrix form as illustrated in Eq. (45).

$$\begin{bmatrix} y_\Delta \\ z \\ E \end{bmatrix} = [P] \begin{bmatrix} u_\Delta \\ w \\ u \end{bmatrix} \quad (45)$$

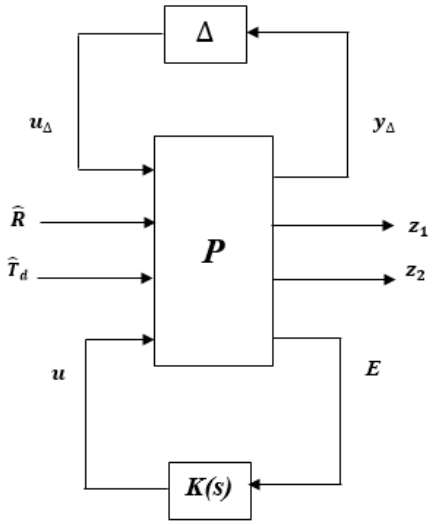

Figure 4: The general control configuration (for controller synthesis)

The exogenous inputs, *w*, and outputs, *z*, are given in Eq. (46).

$$w = \begin{bmatrix} \hat{R} \\ \hat{T}_d \end{bmatrix} \quad z = \begin{bmatrix} z_1 \\ z_2 \end{bmatrix} \tag{46}$$

The P matrix is demonstrated in Eq. (48) and its elements, P11, P12, P21, and P22 are given in Eq. (47).

$$P = \begin{bmatrix} P11 & P12 \\ P21 & P22 \end{bmatrix} \tag{47}$$

$$P11 = \begin{bmatrix} 0 & 0 & 0 \\ -Gw_P & w_P & -G_d w_P \\ 0 & 0 & 0 \end{bmatrix},$$

$$P12 = \begin{bmatrix} w_I \\ -Gw_P \\ w_u \end{bmatrix}, P21 = [-G \quad 1 \quad -G_d], P22 = [-G] \tag{48}$$

the structured matrix $\hat{\Delta}$ is taken into account. The structured matrix is defined, as shown in Eq. (49):

$$\hat{\Delta} = \begin{bmatrix} \Delta & 0 \\ 0 & \Delta_P \end{bmatrix} \tag{49}$$

Figure 5 shows that the uncertainty of the model (Δ) has a single input (y_Δ) and a single output (u_Δ), while the uncertainty of the performance model (Δ_p) has two inputs (z_1, z_2) and two outputs ($\hat{R}$, $\hat{T}_d$). The controller *K(s)* has a single input (*E*) and a single output (*u*).

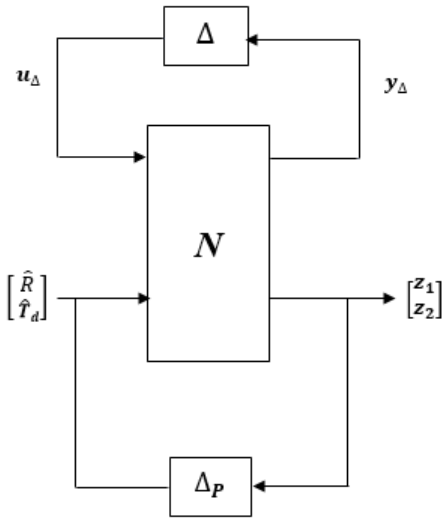

Figure 5: The N-Δ structure.

The system nominal matrix, *N*, shown in Fig. (4) can be written as follows,

$$N = P_{11} + P_{12}K(I - P_{22})^{-1}P_{21} \tag{50}$$

The matrix *N* can be written in terms of its inputs and outputs as shown in Eq. (51).

$$\begin{bmatrix} y_\Delta \\ z_1 \\ z_1 \end{bmatrix} = [N] \begin{bmatrix} u_\Delta \\ \hat{R} \\ \hat{T}_d \end{bmatrix} \tag{51}$$

N matrix can be partitioned into (*N11, N22, N21* and *N22*). The stability and performance criteria are:

Nominal stability (NS): This is achieved when the nominal system is stable without taking the uncertainties into account.

Nominal performance (NP): This is achieved when the nominal system is not only stable but also meets the performance requirements without taking the uncertainties into account as shown in Eq. (52).

$$NP \Leftrightarrow \|N_{22}\|_\infty < 1 \tag{52}$$

Robust Stability (RS): It is satisfied when the system is stable despite uncertainties, as shown in Eq.(53).

$$RS \Leftrightarrow \|N_{11}\|_\infty < 1 \tag{53}$$

Robust performance: It is met when the system meets performance requirements for all perturbed plants in the uncertainty set while maintaining nominal stability, as shown in Equation (54).

$$RP \Leftrightarrow \mu(N, \hat{\Delta}) < 1 \tag{54}$$

5. Results and Discussion

Figure 6 shows the multiplicative uncertainty of the inlet throttling speed control system due to variations in the system parameters for a frequency range, as illustrated in Equation (40). Figures 7 and 8 demonstrate that the H∞ controller determined from Equation (37), meet the conditions outlined in Equation (32).

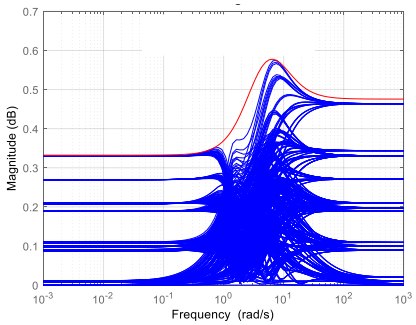

Figure 6: Multiplicative Error transfer function bounding the maximum error

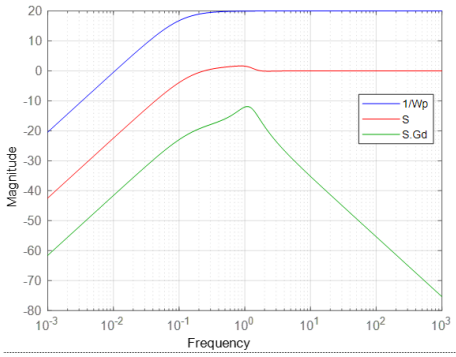

Figure 7: The frequency response of $1/w_p$, S, and S.Gd

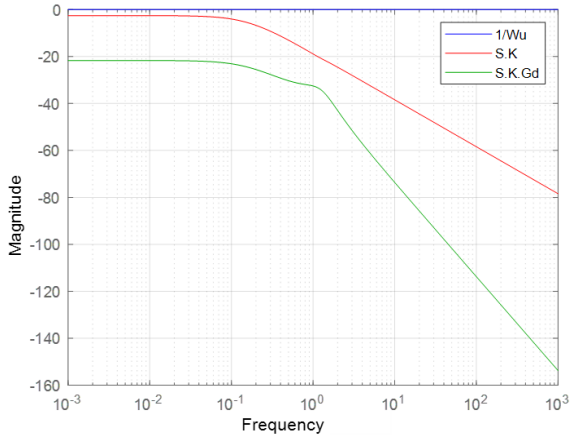

Figure 8: The frequency response $1/w_u$, S.K, and S.K.G_d

Figure 9 shows the time response of the open loop and the closed loop nominal system with PID and H∞ controllers.

The simulations were performed with a unit step of the reference, R̂, at zero time constant and unit step of the disturbance torque, $\hat{T}_d$, at 35 time constants. It is noticed that both the PID and H∞ greatly enhance the system performance. In addition, it can be seen that there is a trade off in the system response, while PID has lower rising time, it has oscillations and overshoot. The H∞ control has another potential advantage which is the robustness that the PID controller does not satisfy. Figure 10 shows the time response of the uncertain system with multiplicative uncertainty. The uncertainties were determined based on errors in uncertain parameters of nominal system within the range of ±10% of their nominal values. It can be noticed that the system has excellent performance within the whole uncertainty set. Note that the real time is calculated by multiplying the dimensionless time by the time constant.

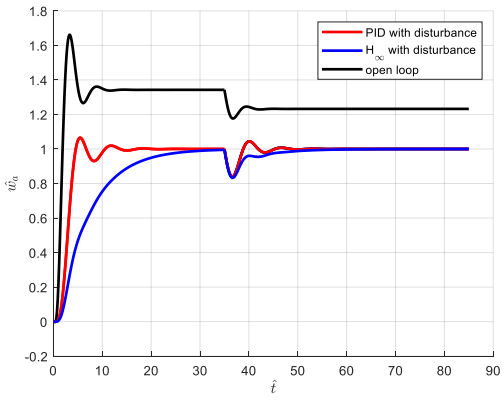

Figure 9: The velocity time response for closed-loop with PID and H_∞ controllers with torque disturbances

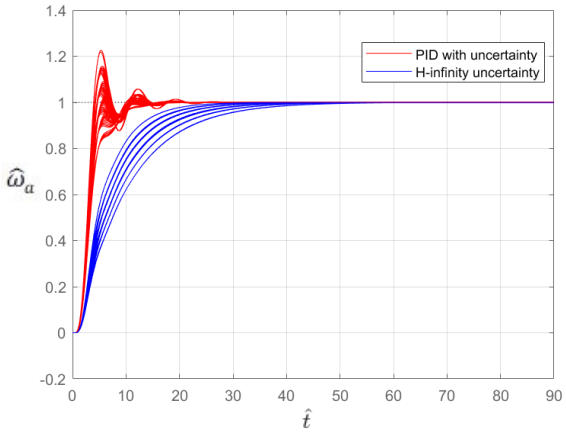

Figure 10: The perturbed velocity time response for closed-loop with PID and H_∞ controllers

Figures 11-13 show the requirements described in Equations (52-54). Figure (11) shows that the both the PID and H∞ controllers meet in nominal stability and robust stability requirements where $\|N_{11}\|_\infty$ for each controller is less than 1 over the entire frequency range. In addition, both controllers satisfy the nominal performance as shown in Figure 12. However, only the H∞ satisfies the robust performance condition as illustrated in Figure. 13.

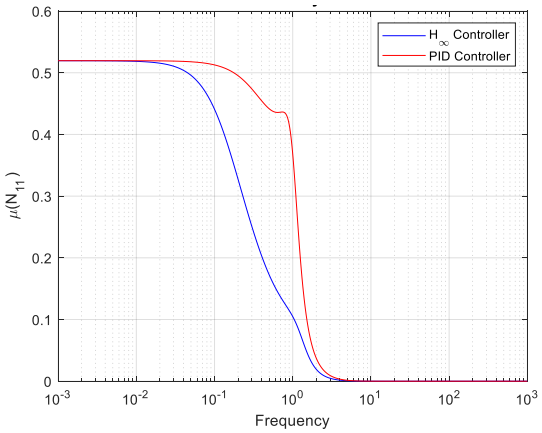

Figure 11: The robust stability requirement

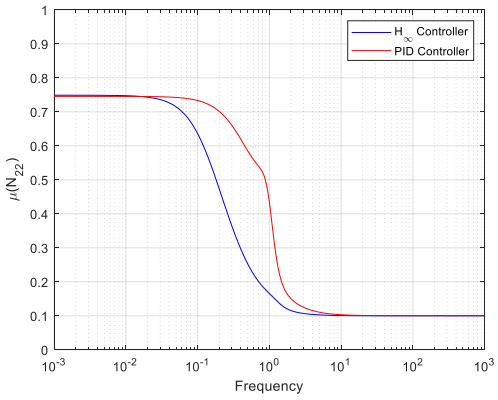

Figure 12: The system nominal performance requirement

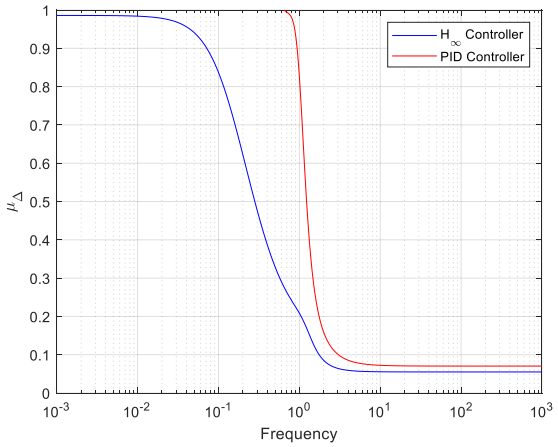

Figure 13: The system robust performance requirement

6. Conclusions

An inlet throttling velocity control system was design and studied in this work with a parametric uncertainty consideration. The system has been modeled and the system stability and performance were assessed for the open loop and feedback control cases. In the closed loop design, PID and H∞ controllers were designed. The system stability and performance have been investigated and compared for the three cases (open loop, closed loop with PID controller, feedback with H∞ controller). It can be noticed that both the PID and H∞ controllers enhance the system performance. The H∞ controller has the advantages of having zero percent overshoot, no oscillations, and no pure integral term that makes it suitable to be used without the needs to anti-windup strategies. In addition, only the H∞ meets the robustness requirements.

Table (2): The definitions of Dimensional Quantity

Dimensional Quantity	NOMENCLATURE
A_v	Opening Area of the Inlet Throttling Valve
a	Maximum Low-Frequency Error
b	Viscous Damping Coefficient
E	Error Signal
G	Nominal Plant Transfer Function
G_d	Disturbance Transfer function
G_{pert}	Perturbed Plant Transfer Function
G_v	Valve Transfer Function
k_1	Leakage Coefficient
k_v	Valve Static Gain
l_I	Multiplicative Uncertainty
M	Maximum High-Frequency Error
J	Mass moment of inertia
P	Pressure
R	Reference Signal
t_d	Valve Time Delay
V_o	Actuator Volume
ω	Actuator Angular Velocity
w	Exogenous Input
w_I	Uncertainty Weight
w_P	Performance weight
w_u	control effort weight
z	Exogenous Output
$z1$	Weighted Performance
$z2$	Weighted Control Effort
η_{at}	Actuator mechanical Efficiency
β	Fluid Bulk Modulus
ω_b	Bandwidth Frequency
ω_n	Valve Natural Frequency
τ	Time Constant
ξ	Damping Ratio of the Valve
ξ_1	Dimensionless Group
ξ_2	Dimensionless Group

References

[1] Ali, Hasan, J. Wisch, R. Fales, and N. Manring, "Efficiency of a Fixed Displacement Pump with Flow Control Using an Inlet Metering Valve," ASME. J. Dyn. Sys., Meas., Control. 141(3), March 2019. doi:10.1115/1.4041606.

[2] Ali, Hasan, R. Fales, and N. Manring. "Design of a Velocity Control System Using an Inlet Metered Pump." Bath/ASME Symposium on Fluid Power and Motion Control (FPMC 2017). Sarasota, FL. Oct. 16–19, 2017.

[3] Triet Hung HO and Kyoung Kwan AHN, *"Modeling and simulation of hydrostatic transmission system with energy regeneration using hydraulic accumulator"*, Journal of Mechanical Science and Technology 24 (5) (2010) 1163~1175.

[4] Ali H, Fales R (2020) "Robust control design for an inlet metering velocity control system of a linear hydraulic actuator". Int J Fluid Power. https://doi.org/10.13052 /ijfp1439-9776.2113.

[5] Zhang, Qin., 1999, "Hydraulic Linear Actuator Velocity Control Using a Feedforward-plus-PID Control," International Journal of Flexible Automation and Integrated Manufacturing, Vol.7, No. 3, pp. 277-292.

[6] Ali, Hasan H., Salwan Obaid Waheed Khafaji, and Fawaz F. Al-Bakri. "H∞ loop shaping control design of the rotational velocity of a hydraulic motor." International Journal of Mechatronics and Applied Mechanics 10 (2021): 72-79.

[7] Pandeli Borodani, Davide Colombo, Marco Forestello, Riccardo Morselli, Patrizio Turco," Robust Control of a New Electro-Hydraulic Pump for Agricultural Tractors". Proceedings of the

18th World Congress The International Federation of Automatic Control Milano (Italy) August 28 - September 2, 2011.
[8] Roger Fales and Atul Kelkar," Robust Control Design for a Wheel Loader Using Mixed Sensitivity H-infinity and Feedback Linearization Based Methods", 2005 American Control Conference June 8-10, 2005. Portland, OR, USA
[9] Arlene Davidson Ra, Dr. S. Ushakumari," H-Infinity Loop-Shaping Controller for Load Frequency Control of a Deregulated Power System", Procedia Technology 25 (2016) 775 – 784.
[10] Coombs, D., 2012, "Hydraulic Efficiency of a Hydrostatic Transmission with a Variable Displacement Pump and Motor," M.S. Thesis, University of Missouri-Columbia.
[11] Ali, H., "Inlet Metering Pump Analysis and Experimental Evaluation with Application for Flow Control," Ph.D. Dissertation, University of Missouri-Columbia, 2017.
[12] Swapnil Pramod Kanade, Abraham T Mathew," 2 DOF H- Infinity Loop Shaping Robust Control for Rocket Attitude Stabilization".International Journal of Aerospace Sciences 2013, 2(3): 71-91 DOI: 10.5923/j.aerospace.20130203.02
[13] Nadir Abbas, Ali Zar , Abdur Raheem , Rabia Shakoor , Zeeshan Ahmad Arfeen , Muhammad Rashid , Farhana Umer , Nouman Safdar ." H∞ Model Based Control via Mixed Sensitivity for 2DOF Control of Twin Rotor MIMO System With Experimental Validation", https://doi.org/10.21203/rs.3.rs-1281134/v1.
[14] Natchanon Chitsanga and Somyot Kaitwanidvilai," 2DOF H infinity Control for DC Motor Using Genetic Algorithms",Proceedings of the International MultiConference of Engineers and Computer Scientists 2014 Vol I, IMECS 2014, March 12 - 14, 2014, Hong Kong
[15] Hasan H. Ali, Ahmed W. Mustafa, Fawaz F. Al-Bakri," A new control design and robustness analysis of a variable speed hydrostatic transmission used to control the velocity of a hydraulic cylinder", International Journal of Dynamics and Control https://doi.org/10.1007/s40435-020-00716-w.
[16] D. J. Hoyle, R. A. Hyde, D. J. N. Limebeer," AN H-infinity, APPROACH TO TWO DEGREE OF FREEDOM DESIGN", Proceedings of the 30th Conference on Decision and Control Brighton, England.December 1991.
[17] Ali HH, Fales RC, Manring ND (2019) Modeling and control design for an inlet metering valve-controlled pump used to control actuator velocity via H-infinity and two-degrees-of- freedom methods. https://doi.org/10.1115/1.4044182.
[18] Ali, Hasan H., Firas M. Abdulsattar, and Ahmed W. Mustafa. "A New Mechanical Analysis of a Crankshaft-connecting Rod Dynamics Using Lagrange's Trigonometric Identities." Journal of Engineering & Technological Sciences 54, no. 2 (2022).
[19] Mannring, N. D., "Hydraulic control systems," Wiley, 2005.
[20] Herbert E. Merritt, "Hydraulic control systems," John Wiley &Sons, Inc, 1967.
[21] Liu-Hsu Lin, Fu-Cheng Wang, *Member, IEEE,* and Jia-Yush Yen *Member, IEEE*," Robust PID Controller Design Using Particle Swarm Optimization", Proceedings of the 7th Asian Control Conference, $\boldsymbol{w_p}\hat{R} - G_d\boldsymbol{w_p}\,\hat{T}_d - G\boldsymbol{w_p}u$ Hong Kong, China, August 27-29, 2009.
[22] Sigurd Skogesad, Ian Post Let hawaite, "MULTIVARIABLE FEEDBACK CONTROL Analysis and design",Second Edition. This version: August 29, 2001
[23] Da-Wei Gu, Petko H. Petkov, Mihail M. Konstantinov," Robust Control Design with MATLAB",Second Edition.
[24] Kemin Zhou, "ESSENTIALS OF ROBUST CONTROL", May 25, 1999